UNIVERSITY OF MINNESOTA
ST. ANTHONY FALLS HYDRAULIC LABORATORY

Project Report No. 105

Comparative Studies of Drop Impingement Erosion and Cavitation Erosion

by
JOHN F. RIPKEN

This research was jointly sponsored by the Fluid Dynamics Branch of the Office of Naval Research and the Naval Ship Systems Command General Hydromechanics Research Program Subproject SR 009 01 01, administered by the Naval Ship Research and Development Center under Contract Nonr 710(72).

APRIL 1969
MINNEAPOLIS, MINNESOTA

ABSTRACT

It has been theorized that the fundamental mechanism of cavitation erosion was essentially the same as that of impingement erosion. The tests conducted in this study were intended to provide additional cavitation and impingement data to support this theory. The tests were conducted on three materials supplied for an ASTM round-robin cavitation test program.

Complete cavitation tests and limited impingement tests on the three ASTM materials are described together with test data on two other metals. Further descriptive material on details for impingement testing is also included.

Only a limited comparison of cavitation and impingement erosion was possible with the data available. This suggests that accelerated laboratory erosion tests may, in fact, over-accelerate the erosion to such an extent that it is not possible to tie the observed erosion to the prototype problem.

CONTENTS

LIST OF ILLUSTRATIONS

COMPARATIVE STUDIES OF DROP IMPINGEMENT EROSION AND CAVITATION EROSION

I. INTRODUCTION

A new type of test facility for simulating impingement and cavitation damage was developed in an earlier phase of this research study, and the facility and preliminary tests therein are described in References [1]* and [2]. The design objective of this facility was to provide a controlled means of maintaining repeated impact between selected liquid drops and a selected solid test specimen in order to establish the erosion characteristics of the solid material. The impact processes employed and the resulting erosion are believed to be a fairly fundamental simulation of the basic mechanism involved in cavitation erosion with the advantage that the significant test variables are amenable to much more rigorous control in an impingement test than they are in an accelerated cavitation erosion test.

The facility consisted of a rotor with a material specimen attached at the periphery in such a manner that there was repeated impact with a column of liquid drops during high-speed rotation of the specimen in a vacuum.

The purpose of the current study was to upgrade certain characteristics of the original rotary impact facility so as to enhance control of the impingement mechanism and to then conduct comparative tests on selected materials in order to better relate the impingement and cavitation processes of erosion. The report which follows consists of description and discussion of (a) findings relating to the impingement facility, (b) results of erosion tests on the selected materials in a vibratory cavitation facility, and (c) results of limited erosion tests conducted in the improved impingement facility.

Fortunately, the test program was conducted concurrently with a round-robin cavitation erosion study carried out under the auspices of Committee G-2 of the American Society for Testing and Materials. The Committee provided most of the test materials for this study. The materials came from

*Numbers in brackets refer to the List of References on page 21.

a common source, and cavitation erosion studies were conducted on these same materials by ten other laboratories.

The use of these materials in the current study will ultimately provide comparative data which may contribute to a much broader understanding of erosion test methods.

II. THE IMPROVED ROTARY IMPACT FACILITY

The tests described in Ref. [2] pinpointed a number of deficiencies in the initial facility. Most of these deficiencies related to the control and evaluation of the characteristics of the water drops from which the entire erosion process stems, and thus a substantial portion of the contract funds was allocated to improvement of the facility. The following items discuss separately various characteristics of the facility after the improvement program.

A. Water Drop Size

Degassed, distilled water was delivered to the impact target in drops which could be kept essentially constant in size throughout a given test program. This size was in the range from 0.5 to 0.9 mm. Since the drop generator is synchronized to the rotor speed, the exact size depends slightly on the desired test speed. An exact size cannot be predetermined to specification, but can be approximated and then measured with fair precision using a small, calibrated, in-line rotameter which gages the rate of flow of the water fed to the generator. A concurrent accurate electronic count of the rate of drop generation permits the mass of the drop to be known within five per cent. From the established mass of the drop, the size can be calculated quite accurately.

B. Water Drop Shape

Due to surface tension effects, the water drop experiences oscillatory shape changes immediately after formation at the terminus of the capillary tube of the generator. These oscillations are rapidly damped out in the vertical fall distance between the drop generator and the point of impact. High-speed photos of the drop taken during the approach of the target

indicate that the drop remains stable and essentially spherical in shape right up to the instant of impact with the target.

C. Target Velocity

The target velocity is calculated from the relation $V_t = 2\pi RN/60$ where

V_t = target velocity in fps

R = radial distance from center of target to center of rotation = 0.987 ft

N = shaft rotation in rpm

The shaft rotary speed was infinitely variable through manual adjustment of a variable speed electric motor. The shaft speed was read with an electronic counter which sampled the rate of rotation as a function of the rate of triggering of a photoelectric cell by a light beam actuated by a slotted drum attached to the rotor. The electronic counter repeatedly sampled the count each second and provided a digital display of the N value. The motor speed was adjusted to give an N count consistent with the V_t value desired from the equation. Once adjusted, the speed remained quite stable.

D. Drop Alignment and Count

Generation of the drops, which was activated essentially by synchronizing with the shaft rpm, was initiated following stabilization of the target velocity. Alignment of the drop with the target center was accomplished by manual adjustment of positions. The adjustment was approximated quite closely while the generated drop stream descended clear of the rotor tip. When alignment had been achieved, drops were electrostatically deflected into the path of the target. This deflection was initiated manually and continued once per revolution up to some pre-selected value x, which was programmed into a second electronic counter system. The deflection then continued automatically until the pre-set count was completed or until the operator manually interrupted the deflections. The operator continually observed the impingement through a telescope and normally allowed the count to proceed unless he observed excessive drift in the impact location or

other abnormalities in the generator action. When this occurred, he could interrupt the deflection and realign the drop impact point. Once realigned, the deflection could be reestablished and the impingement count continued. The electronic counter retained the number of impacts during any given interruption and picked up and continued the count when the deflection was reestablished. The number of drops delivered to the target could be manually controlled for a selected elapsed time or pre-selected for electronic counting and control in groups of 1000 to groups of 100,000. Lower and higher numbers could also be obtained without full automatic control. The control was such that the delivered number of drops could be known with an error considerably under one per cent.

E. Impinged Area of Target

The question of whether the drops should be delivered at one point on the target or randomly over a selected area was debated. In this case preference was given to simplifying the geometry by delivering at a single point. However, slight instabilities in the drop generator and windage or compressibility effects from the rotor normally produced a slight wandering about the desired target point. The operator continually observed through a telescope the target face during impact and manually adjusted the generator to maintain the impacts within a selected circle of resolution. This circle was very stable at approximately one drop diameter for target velocities below about 750 fps and could readily be adjusted to stay within about two drop diameters at about 1000 fps. However, at velocities around 1200 fps this dispersion circle grew to almost the full 1/4-inch diameter of the target face and was difficult to reduce below this value. In the current tests the velocity was held at 1000 fps with an impingement area of two diameters. The loss of some control above 1000 fps was believed due to compressibility shock wave effects generated by the rotor operating in the confined chamber. Control improved with a lower vacuum in the chamber, but the vacuum was limited by the evidence of boiling on the water drops. It appears that these effects will serve to limit the absolute velocities that can be achieved in this type of apparatus. A simulation of higher velocity impact conditions might, however, be achieved through the use of liquids having density or compressibility values significantly greater than those of water.

F. Drop Splash

High-speed single-flash photos were taken of the impact phenomena, but are not of sufficient quality for reproduction herein, nor do they allow analysis of relative velocities. Study of these photos and the somewhat related photos of Fyall [3] does, however, suggest that the initial lateral liquid flow following impact does not occur in a purely radial direction along the face of the specimen, but possesses an additional component normal to the specimen face.

The normal component evidently stems from some elastic recovery or rebound from the compression of the water and the compression of the specimen. The initial flow is thus along the surface of a cone of considerable angle with the target face. Fyall [3] measured the initial radial component of velocity as being about three times that of the impact velocity. The photos made in connection with these tests, which were taken at a somewhat different angle than Fyall's, show that the conical flow is not a solid sheet, but--due to surface tension forces--breaks down, almost at the edge of the impacting drop, into a sunburst composed of a great many small drops and jets.

The latter observations in combination with Fyall's data and photos suggest that the lateral flow may have two discrete phases, the first of which is the spray cone of very high velocity, with the second phase being a more nearly radial flow at a lower velocity. The initial conical flow presumably results from the high impact pressure ($p = \rho cV$), whereas the later radial flow results from the much smaller stagnation pressure ($p = \rho V^2/2$) which follows the impact pressure.

G. Depth of Target Erosion

Erosion of material in the impact facility was confined to a relatively small target area (slightly more than one drop diameter) and progressed as a hole of increasing depth but with relatively little increase in diameter. Erosion tests were therefore terminal when the depth extended through the target material. In earlier tests the target thickness in the erosion area was approximately 1/16 inch, but in later tests this was increased to 3/32 inch. Greater thicknesses were not attempted, because the initial erosion is considered more generally significant than erosion at depth. Greater

thickness also imposed greater centrifugal forces on the shank supporting the head, as evidenced by the bending of the head in tests with low-strength ductile materials.

H. Ambient Test Pressure

The impact occurred within a closed housing container, and during tests the interior pressure was reduced by a vacuum pump. Reduced pressure was necessary to reduce air density and the resulting aerodynamic drag on the rotor. In earlier tests the pressure was reduced to about 1/100 of the existing exterior atmospheric pressure (0.01 A), but pressures were subsequently increased to 0.02 A due to evidence of instability of the drop surface, which was presumed to approach boiling. A pressure lower than about 0.03 A was necessary for proper action of the high-voltage drop deflector circuit.

I. Ambient Test Temperature

Spray created by drop impact densified the chamber atmosphere and fogged visual observation of the target. A refrigerated heat exchanger mounted on the floor of the housing condensed most of the fog and maintained a low freezing temperature of about $10^{\circ}F$ on all interior walls. The drop generator expelled drops at essentially room temperature, but the drop and target temperatures at the time of impact are unknown. At speeds below 500 fps, target temperature was evidently below freezing, since ice was observed to form on it. Above 500 fps ice was not apparent.

III. THE VIBRATORY CAVITATION EROSION TESTS

A. Objectives

The cavitation erosion tests described herein were the first part of a two-part program intended to bring about a better understanding of the relationship between cavitation erosion processes and impingement erosion processes. In addition to this comparative use, the cavitation tests were also intended to serve as part of a round-robin cavitation erosion study conducted under the auspices of Committee G-2 of the American Society for Testing and Materials. The latter study had the objective of establishing a new

preferred standard for future evaluation of the erosion character of various engineering materials. The study program called for cavitation erosion tests in the vibratory erosion facilities of eleven different laboratories using three selected common materials. The tests have now been completed, and the individual findings of a number of the laboratories are reported in References [4], [5], and [6]. A preliminary summary of the findings is contained in [7], and a formal published summary is now in preparation. The present report serves, in part, as a record of the related cavitation erosion tests which were conducted at the St. Anthony Falls Hydraulic Laboratory.

B. Test Materials

For the comparative evaluations, Committee G-2 attempted to select three materials which had a considerable range of erosion resistance and which could be reproduced at a later date with only negligible changes in characteristics. The selected materials were

Aluminum 6061-T-651 (Alcoa designation)
Stainless steel type 316
Pure nickel type 270 (International Nickel Company)

These materials were supplied as bar stock by Committee G-2 from a common source, mill run and heat treatment (unspecified). The properties of these materials are given in Table I.

In addition to the materials supplied by the ASTM Committee, limited tests were also conducted at the St. Anthony Falls Laboratory on samples of alloy steel 4340 and of heat-treated stainless steel 17-4PH. The 4340 steel, a resistant material, was supplied by Dr. Milton Plessett of the California Institute of Technology. Published data are available on tests of this material at Cal Tech. The heat-treated 17-4PH alloy was included because of its recent adoption by the Boeing Company for fabrication of the underwater hydrofoil assemblies of the new PGH-2 hydrofoil ship which Boeing designed, built, and delivered to the Navy. The materials supplied by Boeing were cylinders taken from a 2-inch-thick plate which had been subjected to "Condition A" solution treatment, followed by a four-hour age-hardening treatment at 950°F, and then cooled in air. One specimen had a test surface which was in a plane parallel to the usual surface of the plate, and one had a test

TABLE I. PROPERTIES OF CAVITATION TEST SPECIMENS

MATERIAL:	316 Stainless Steel	270 Nickel	6061-T-651 Al Alloy	4340	17-4PH
Composition - per cent					
C				0.38	0.07
Cr	18		0.25	0.75	15.5-17.5
Ni	13	99.98		1.79	3.0-5.0
Mo	2.5			0.26	
Mn	1.6			0.73	1.0
Fe	bal			bal	bal
Me			1.0		
Si			0.6		1.0
Cu			0.25		3.0-5.0
Al			bal		
Tensile Strength (psi)	81,250	48,750	47,260		170,000
0.2 per cent Yield Strength	31,310	8,000	40,680		150,000
Elongation - per cent	69.0	61.0	21.5		10
Reduction of Area - per cent	76.9	91.5	44.0		44
Hardness	74.8 Rock-B	24.9 Rock-B	60.1 Rock-B	235 B/H (3000)	39 Rock-C
Charpy Impact Ft-Lb	136.0	91.0	5.5		5.0
Density - Gr/cm^3	7.91	8.94	2.71		7.78

surface cut perpendicular to the longitudinal axis of rolling. Unlike the ASTM test specimens, which were machined from solid bar stock greater than 5/8 inch in diameter, the 17-4PH material was available only in a 1/2-inch-diameter rod. This necessitated mounting in a 5/8-inch housing ring to achieve standard specimen dimensions.

C. Cavitation Test Facilities

1. The Vibratory Apparatus

The apparatus was designed to produce a vibratory action approximating that specified by an earlier ASME tentative standard as described in Reference [8]; that is, a nominal frequency of 6500 cps with a peak-to-peak amplitude of 0.004 in. The system was in this case built around a standard Hewlett-Packard Model 200B oscillator whose output was fed into a suitable power amplifier. The output of this amplifier, rated at 200 watts, was fed into a self-cooled magnetostrictive transducer consisting of a wire-wound laminated nickel stack. A mechanically amplifying stainless steel exponential horn was mechanically clamped at its top to the base of the nickel stack and was in turn provided at its lower end with a 5/16-inch-by-32 male thread for specimen attachment as shown in Fig. 1.

Vibration amplitude was monitored during tests through the use of a signal generated by an inductive pick-up coil surrounding the lower end of the exponential horn at a position 2-1/2 inches above the face of the test specimen. The signal was read out with an rms voltmeter which was calibrated under normal use conditions by visually observing the oscillation of highlighted reference marks on the side of the specimen. The motion was observed through a microscope under synchronized strobe lighting. Selected samples of the signal from the inductive pick-up were also recorded photographically from an oscilloscope to yield the wave form of the horn oscillation as typified in Fig. 2. The oscilloscope signal of horn motion is assumed to approximate the nature of the wave form occurring at the specimen face. Figure 2 shows that the wave form of the oscillation does not approximate a good sinusoidal form, but is somewhat more sharply peaked, even for the condition of operation in air. The curve generally appears to be rather erratic in the peak region for the condition of operation in water.

Vibration frequency was measured by the digital read-out of an electronic counter continually displaying a repeating one-second count of the input from the oscillator.

Pretest trials, using normal operating conditions and selected variations of the input oscillator frequency and the output power of the amplifier, determined the preferred operating conditions. For this particular apparatus the most workable approximation to the tentative standards of the ASME [8] was thus established to be a frequency of 5900 $\pm$ 25 cps and a double amplitude of 0.004 in. Continual observer monitoring and adjustment were required to stabilize the amplitude due to frequency drift associated with progressive horn heating.

The apparatus was surrounded by a windowed noise-reducing housing to minimize the ear-damaging acoustic output. In addition, the test operator was required to wear acoustic earmuffs.

2. Test Specimens

The material specimens in these tests were used in the cylindrical form shown in Fig. 1. This configuration conforms to the flat face, vertical sides, and 5/8-inch outside diameter of the face as used in Reference [8]. In other respects the test specimen dimensions were established so as to maintain a small but common specimen weight for all specimens. Constancy of weight was considered desirable in the interest of maintaining an essentially fixed value of the vibratory frequency and amplitude, and a small weight permitted utilization of the highest possible inherent frequency. The initial values of the frequency and the amplitude which prevailed during the tests are given in the graphical data summaries of Figs. 3 through 7.

The SS-17-4PH, which was supplied in 1/2-inch diameter, was provided with an external bushing to achieve the outer diametral dimension shown in Fig. 1. This bushing was threaded to the exterior of the original cylinder materials and rigidly attached by treating the top end of the threads with Loctite Retaining Compound (Loctite Corporation).

Attachment of the test specimen to the vibratory horn employed a 5/16-inch-by-32 thread on the horn mating with a 5/16-inch-deep, square-bottomed, tapped hole in the specimen. The specimen was firmly tightened on the horn

and a light coating of silicone grease was applied to the threads to improve coupling.

3. Test Bath

In accordance with the findings of others [9,10], tests were conducted with the working face of the test specimen immersed 1/8 inch below the static surface of the water in a Pyrex beaker. The beaker was a standard 400 ml size (3 inches in diameter by 4 inches in depth) filled with 350 ml (3.5 inches of depth) of distilled water.

The single-distilled test water was tested for pH value prior to and following each test run. Values were measured with a Beckman glass electrode pH meter.

The temperature of the test water was held at about 75°F by removing the accumulated heat via a water bath surrounding the test beaker. The surrounding water bath consisted of a 4-inch-square tank having a water depth of 4 inches. The water in this bath was continually changed by a small pumped flow from a larger reservoir whose temperature was controlled electrically. Preliminary tests established that at normal room temperatures and following a normalizing vibrator run of one-half hour, the temperature of the test water could be maintained at 75°F $\pm$ 1° by maintenance of a 67°F temperature in the control reservoir. The thermometer measurement of the water temperature was read by inserting the thermometer in the static beaker water.

D. Test Procedures

1. Initial Preparation of Specimens

The test specimens were machined from the material as supplied in accord with the dimensions shown in Fig. 1, with the specification that on the face machining the roughing cut was to be followed by one smooth finishing cut with a sharp tool. The machined face was then surface-ground in light passes until at least 0.002 inches of material were removed, and then wet-finished by hand with No. 320, then No. 400, then No. 600 paper. According to Ref. [10], this operation removes surface materials which may have local work

hardening due to prior machine operations and thus provides a more representative exposure of the material and a more uniform roughness. The surface roughness of the specimens was measured with a roughness meter (Profilometer-Pilotor Micrometrical Manufacturing Company) and was found to range from 3 to 7 micro-inches rms. The specimens were carefully degreased with methyl-ethyl-ketone and xylene before use.

2. Routine Handling of Specimens

Test handling of the specimens involved cleaning and then weighing. The principal objective of the cleaning was the removal of all loose metallic debris, grease, and free water from all exterior surfaces. The removal was accomplished by first degreasing in a solution of methyl-ethyl-ketone and xylene, then rinsing in distilled water, and finally drying in a clean, dry air blast. Because of the threaded fabrication of the 17-4PH specimens, these units were heated for 15 minutes at 110°C for final moisture removal.

Weighing was then carried out on an analytical balance which had been checked to assure weight measurements to $\pm$ 0.1 milligrams.

This procedure was repeated after every step in a test program consisting of a series of tests and weighings. The increments of test time were arbitrarily selected to provide an erosion weight loss record of the desired form.

3. Normalizing Pre-Run Procedures

In order that all tests might be conducted under uniform conditions, the vibratory apparatus and test bath were initially exposed to a one-half-hour pre-test run using a dummy specimen. The purpose of this run was to normalize the temperature and output values of the vibratory apparatus and to precondition the gas content [9,10] and thermal values of the test bath. These same values were also maintained between the separate steps of a test by installing the dummy specimen and operating the apparatus whenever the down-time exceeded a few minutes.

To minimize erosion on the dummy, these units, which were made of 304 stainless steel, were given a commercial hardfacing overlay (Eutectic Welding Alloys Corporation Borotec 10009).

E. Test Data

The data on time versus weight loss have been graphed separately for each of the selected metals in Figs. 3 through 7. For each of the three ASTM metals two separate specimens were tested. One of these was subjected to tests with relatively small exposure time increments and the other was run in a check test using larger time increments. In addition to the plottings of time versus weight, the data have been subjected to a numerical differentiation procedure so that erosion loss could be expressed as a rate. The rate of loss has been plotted separately using the alternate ordinate scale on the right-hand side of the figure in units of milligrams per minute (arbitrarily chosen).

The duration of the test for each material was established by progressively plotting the time-weight loss values until the data gave evidence that a steady rate of weight loss had definitely been achieved or exceeded. This steady region is the peak between the "accumulation zone 2" and the "attenuation zone 3" described in Ref. [9] and is referred to as "Phase 3" in Ref. [11].

In addition to the erosion data values which are plotted in Figs. 3 through 7, small separate sketches have been added at the tops of the figures to show the area of the specimen face over which erosion took place at various times in the erosion sequence. Figure 3 shows a typical erosion sequence in which after 30 minutes erosion was observed as a slight etching of the specimen surface within the small (shaded) circle at the center. This was surrounded by a small circular band of undamaged surface and an additional outer (shaded) narrow band of damaged surface. From the latter band to the outer edge of the specimen there was no evident damage. As time progressed the separate etched areas gradually merged into one large etched circle (shaded), as shown at 90 minutes in Fig. 3. As time passed, the diameter of the etched area grew progressively greater and a deeper erosion was superimposed on part of the etched area (x-hatched). These erosion sketches, as shown above the erosion-time curves of Figs. 3, 4, 5, and 7, are drawn to approximately full scale with the outer diameter being the 5/8-inch specimen face. The erosion pattern at the termination of testing was a shallow dish-shaped depression with a generally small-scaled roughness on which deeper circular grooves of erosion were superimposed.

On the nickel, the 316 stainless steel, and the 4340 steel the deeper areas of erosion were somewhat rougher in texture than the background, and this texture consisted of short ridges. On the 17-4PH stainless steel the eroded areas were similar to the foregoing, but much smoother and flatter in texture. On the aluminum the erosion consisted of deeper dimples. The conditions of the surfaces of the three ASTM materials at the termination of testing are shown in photographs in Ref. [7]. In addition to the weight-loss data and the erosion sketches, the data figures include notations giving the pH value of the test water before and after testing and the atmospheric pressure at the time of each test.

F. Summary of Cavitation Erosion Findings

The general materials ranking and character of the erosion losses experienced in these tests were similar to those experienced by most of the other reporting laboratories as summarized in Ref. [7]. This similarity exists despite the fact that the St. Anthony Falls tests represented the facility of lowest vibratory frequency. The lower frequency generally, but not consistently, produced a somewhat lower weight loss per unit of time than did the higher frequency.

Examination of the comparative area of erosion in Figs. 3 through 7 indicates that this value is a function of both the type of material and the duration of exposure. This is a significant variable if a parameter such as "mean depth of penetration" is to be used for data comparison. In the St. Anthony Falls tests with a low frequency ($\approx$ 6000 cps) the maximum eroded area varied from about 30 to 42 per cent of the face area for the different materials when run through the "accumulation zone" of a test. A similar zone of duration in some of the intermediate-frequency facilities provided eroded areas of 60 to 80 per cent of the total, whereas with the higher-frequency facilities erosion generally covered more than 90 per cent of the total area.

Tests of the 17-4PH stainless steel are interesting in that they demonstrate the marked difference in erosion that may result for the same material when the grain structure is presented to the erosive force system in a different orientation. This suggests that standardized procedures for conducting tests should specify or give consideration to any asymmetrical properties that the material may possess. The evidence in Ref. [7] of different erosion losses

for repeated tests of the same material in the same facility and differences for the same material in similar facilities may be due in part to differences in orientation. There is no evidence in any of the tests of Refs. [4], [5], and [6] or in those at the St. Anthony Falls laboratory that a consistent orientation of material was employed in fabricating the test specimens.

The test of the 17-4PH stainless steel is also interesting in that one of the specimens exhibited the highest rate of erosion near the beginning of the test, whereas the other specimen peaked out in a more conventional manner. Since these tests involved only one specimen for each sample of metal and of necessity employed a two-piece specimen mounting, the evidence may not be conclusive.

IV. THE IMPINGEMENT EROSION TESTS

A. Test Materials

It was intended to conduct the impingement erosion tests on the three metals supplied by the ASTM Committee. Unfortunately, these tests were conducted late in the Navy-sponsored program, and the available funding limited the tests to a small number of the 316 stainless steel specimens.

In a subsequent but different program conducted for the General Electric Company, Missile and Space Division, under a contract with NASA, impingement erosion tests were conducted on several metals. These tests included a Nickel 270 which was basically the same as the pure nickel that was supplied by the ASTM Committee and tested in the vibratory cavitation facility. In this case, however, the metal came from a different source and was subjected to a heat treatment of one hour at 900°F prior to the test. The physical characteristics of this material and the preparation of the specimen are to be described in detail in a separate report covering the General Electric Company program by Dr. O. G. Engel of General Electric.

B. Test Procedures

The impingement erosion tests were quite similar in intent to the tests in the vibratory cavitation erosion facility in that erosive weight loss was measured as a function of time or number of impacts. The procedures employed in the tests were essentially those described in Ref. [2] and in the earlier

portions of this report, with one major exception: In these impingement tests of the 316 stainless steel and the 270 nickel, each test point was run with a different test specimen instead of the same specimen being used at all points and accumulating the erosive loss. This procedure introduced the possibility of differences among the specimens due to possible slight fabrication variations, and may have caused some scatter in the resulting test data, but such scatter should not be any greater than would have resulted in repeated cumulative tests on various specimens. The prime advantage of using individual specimens is that they can be permanently retained for sectioning, micro-examination, etc.

C. Test Data

For the 316 stainless steel, test runs were made at impingement velocities of 750, 1000, and 1250 fps. The tests at 750 fps failed to show any evidence of erosion for exposures up to 1×10^6 impacts, so the test was terminated.

Tests at 1000 fps first gave evidence of erosion at about 1×10^5 impacts, and tests were continued to 3×10^5 impacts, where they were terminated because the maximum rate of loss had evidently been exceeded.

Tests at 1250 fps first gave evidence of erosion at about 6×10^4 impacts. Only three tests had been completed at the time of termination of the test program.

The weight loss data for the tests of 316 stainless at 1000 and 1250 fps are plotted in Fig. 8.

For the 270 nickel, test runs were made only at 1000 fps, and the tests were continued until the erosion hole extended through the full thickness (about 3/32 inch) of the head of the specimen. The weight loss data for this metal are shown in Fig. 9.

It should be noted that the loss data for this metal are considerably more irregular than for several other metals which were tested in the General Electric Company program. The irregularity is thus believed to represent some inherent variability of the specimens rather than abnormalities in the testing procedures. This irregularity was evident also in the incubation conditions, which for four different specimens were observed to vary from about 1600 impacts to about 6400 impacts.

D. Summary of Impingement Erosion Findings

Unfortunately, limited funding did not permit the completion of full erosion test curves for the ASTM materials in the impingement test facility to allow detailed comparison with the ASTM erosion tests in the vibratory cavitation facility. The limited data of Figs. 8 and 9 do, however, indicate the need for additional studies. These studies should include comparative runs to clarify whether the observed scattering of test values is due to inherent variation in the basic material, variations in preparation of the specimens, or variations in the impingement mechanism. Such studies should also include the completion of test curves using both individual specimens per test point and single specimens with progressively accumulated erosion. Special care should be taken to see that specimens are prepared with a common orientation relative to the original rolling of the material to avoid the possible contributions found in the cavitation tests of the 17-4PH stainless steel, shown in Fig. 7.

It is interesting to note that the ASTM tests reported on in Ref. [7] include impingement erosion tests by the Laboratory of Electricité de France. The impingement facility in that case used specimens mounted on the periphery of a rotating disk. The rotation passed the specimens through a small water jet at a rate of 2900 times a minute with a resulting impingement velocity of 312 fps. The erosive weight loss curves for the ASTM 316 stainless and 270 nickel are reproduced here as Figs. 10 and 11. The curves are significant when compared to Figs. 8 and 9 in that they demonstrate the marked influence of heat treatment and the need for more rigorous control and specification of pre-test treatments in studies such as those described in Ref. [7].

V. COMPARISON OF CAVITATION AND IMPINGEMENT EROSION TESTS

Although the available impact tests are limited in number and varied in the materials involved, certain comparisons can be attempted for the cavitation erosion tests and the impingement erosion tests. For example, the 316 stainless steel cavitation erosion data shown in Fig. 3 can be compared with the impingement erosion data in Figs. 8 and 10. In all instances the general trend of erosion is similar for this material in that a distinct "incubation" period is evident prior to actual erosion. However, in the case of cavitation

the initial erosion appears to have been much more gradual than for either of the impingement tests. For the latter, the rate of erosion became high shortly after erosion began. These markedly different rates may be due in part to the differences in effective erosion area. In the case shown in Fig. 8 the erosion involved an essentially constant area of the test specimen, and it is presumed that this was also approximately the case in the jet erosion tests of Fig. 10 conducted by Electricite de France. However, as shown in the cavitation erosion patterns of Fig. 3, the involved area of erosion increased rapidly during the initial stages of erosion and thus introduced a quite different concept of energy loading values and time factors. While the various forms of vibratory cavitation facilities differ markedly in the stability of the area which they erode, most forms show considerable area variation in the early portions of their weight loss curves. Thus there is reason to doubt the significance and the comparative worth of this portion of the curve.

Comparative tests for erosion of the 270 nickel show some similarity in shape for the cavitation data of Fig. 4 and for the two types of heat treatments employed in the jet impingement erosion tests of Electricite de France as seen in Fig. 11. There is, however, little resemblance to the general shape of the data curve of Fig. 9, which shows no tendency toward "incubation" or erosion delay, but proceeds instead to show immediate erosion on impact. Although the data of Fig. 9 do relate to a different heat treatment of the material than do the data of Figs. 4 and 11, it is perhaps more important to recognize that there are widely different test environment conditions involved here. For example, the tests of Fig. 9 involved drop impingement at a velocity of 1000 fps, whereas those of Fig. 11 involved a velocity of slightly over 300 fps. If the impingement pressure is assumed to be roughly approximated by the value of ρcV, the resulting values for $V = 1000$ fps and $V = 300$ fps are approximately 63,000 psi and 19,000 psi. If these values are compared to the properties of 270 nickel as given in Table I, it is evident that the character of erosion at a velocity of 1000 fps might little resemble the character of erosion at 300 fps.

The available data are too fragmentary to allow analysis in depth, but they do suggest that accelerated laboratory erosion tests may in fact overaccelerate to the extent that the resulting damage shows no clear tie to the erosion mechanisms of the prototype problem.

VI. ACKNOWLEDGMENTS

The writer gratefully acknowledges:

(a) the support of the Office of Naval Research and the Naval Ship Research and Development Center;

(b) Permission to use the test data of Fig. 3 by Dr. O. G. Engel, Missile and Space Division, General Electric Company, under NASA Contract NASW 1481;

(c) Specimens supplied by the G-2 Committee of ASTM, by Dr. M. S. Plesset of the California Institute of Technology, and by Mr. W. R. Wiberg and Mr. F. B. Watson of the Boeing Company; and

(d) The efforts of Dr. J. M. Killen and Mr. J. A. Almo in the development of the facilities and of Mr. T. P. Lentz, Dr. R. M. Olson, and Mr. M. W. McKay in conducting the various tests.

LIST OF REFERENCES

[1] Ripken, J. F.; Killen, J. M.; Crist, S. D.; and Kuha, R. M., A New Facility for Evaluation of Materials Subject to Erosion and Cavitation Damage, Univ. of Minnesota, St. Anthony Falls Hydraulic Laboratory Project Report No. 77, March 1965.

[2] Ripken, J. F., "A Test Rig for Studying Impingement and Cavitation Damage," Erosion by Cavitation or Impingement, American Soc. for Testing and Materials, ASTM Special Technical Publication 408, 1967.

[3] Fyall, A. A., "Single Impact Studies with Liquids and Solids," Proc. of the Second Meersburg Conference on Rain Erosion and Allied Phenomena, August 1967.

[4] Hickling, R. and Orlosky, S. E., Cavitation Damage Measurement for the ASTM Round-Robin Tests, General Motors Corp. Research Publication GMR-784, July 1968.

[5] Marx, V. E., Erosion by Cavitation in an Ultrasonic Vibratory Test Rig for the ASTM Round-Robin Tests, Westinghouse Electric Corp. Engineering Report EM-994, September 1968.

[6] Young, S. G., Cavitation Damage of Stainless Steel, Nickel and an Aluminum Alloy in Water for ASTM Round-Robin Tests, Nat. Aero. and Space Adm. Tech. Memo X-1670, October 1968.

[7] Chao, C., et al., ASTM Round-Robin Test with Vibratory Cavitation and Liquid Impact Facilities, Univ. of Michigan, Dept. of Mechanical Engineering Report No. MMPP-344-3-T, November 1968.

[8] Robinson, L. E.; Holmes, B. A.; and Leith, W. C., "Progress Report on Standardization of the Vibratory-Cavitation Test," Transactions, American Society of Mechanical Engineers, Vol. 80, No. 1, January 1958.

[9] Thiruvengadam, A. and Preiser, H. S., "On Testing Materials for Cavitation Damage Resistance," Journal of Ship Research, Vol. 8, No. 3, 1964.

[10] Hobbs, J. M.; Laird, A.; and Brunton, W. C., Laboratory Evaluation of the Vibratory Cavitation Erosion Test, National Engineering Lab., Report 271, January 1967.

[11] Hobbs, J. M., "Experience with a 20 kc Cavitation Erosion Test," Erosion by Cavitation or Impingement, American Soc. for Testing and Materials, ASTM Special Technical Publication 408, 1967.

F I G U R E S

(1 through 11)

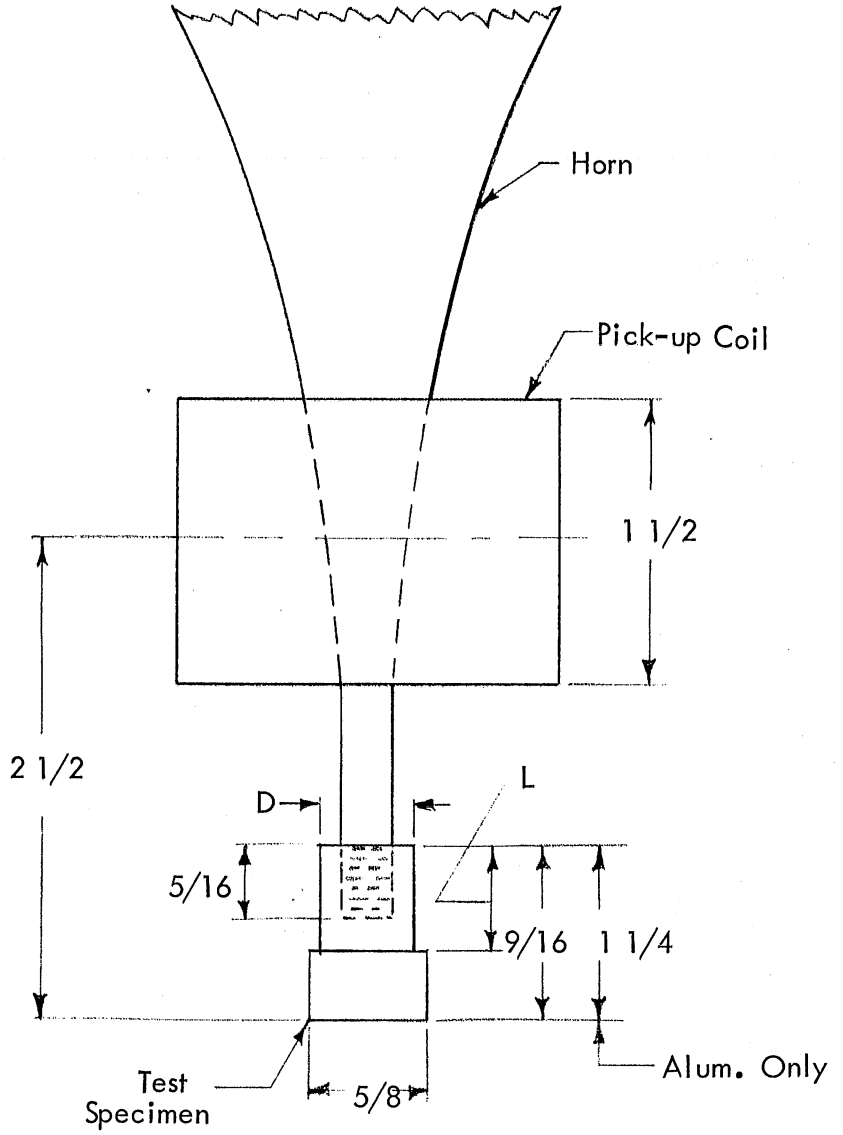

Material	Dimensions		Specific Weight lbs/cu. in.
	L	D	
Nickel 270	5/16"	1/2"	0.321
St. Steel 316	3/16	1/2	0.286
Alum 6061-T	0	5/8	0.098
St. Steel 17-4PH	3/16	1/2	0.287
Steel 4340	11/64	1/2	0.283

Fig. 1 Dimensional Values for Specimen and Horn Extremity

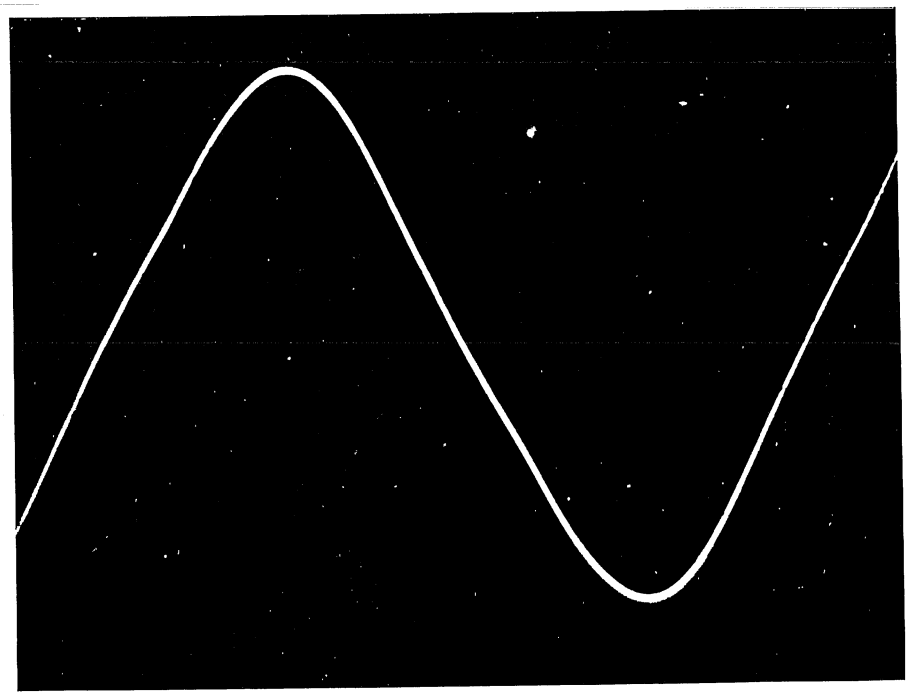

(a) Specimen Oscillating in Air

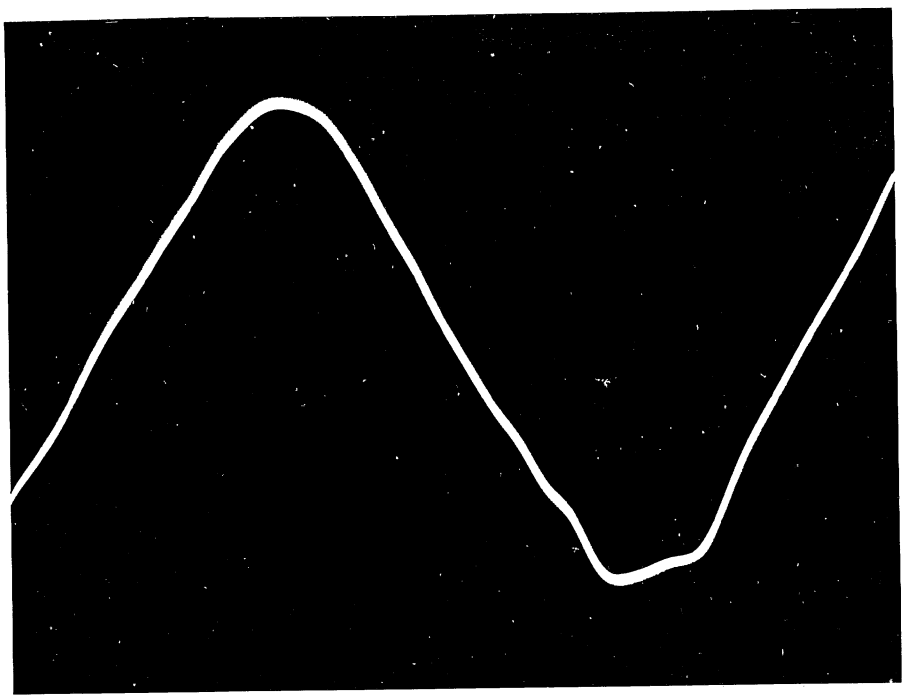

(b) Specimen Face Submerged in Water 1/8 inch

Fig. 2 Typical Oscilloscope Records of the Vertical Oscillation of the Cavitation Test Specimen

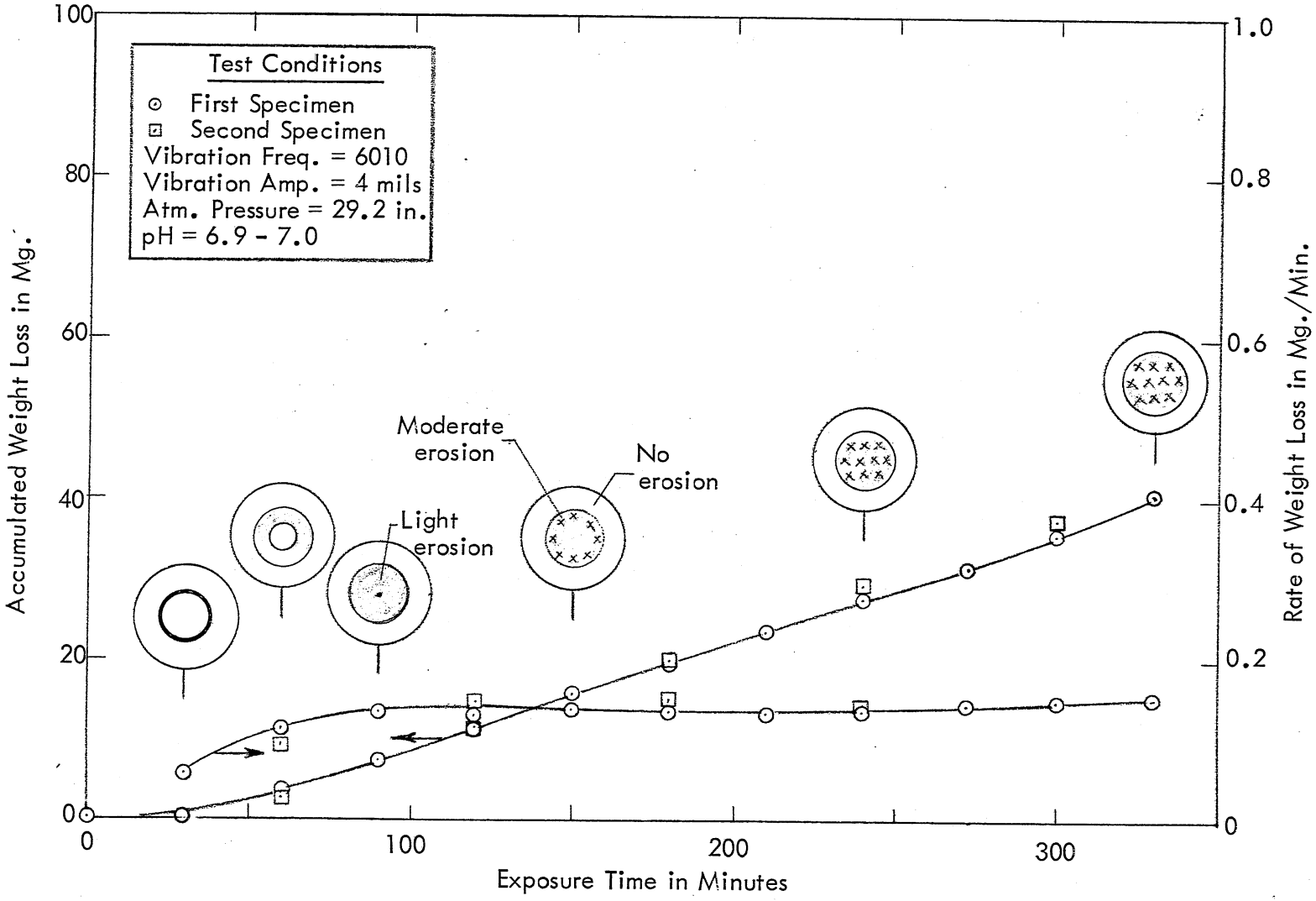

Fig. 3 Cavitation Erosion for 316 Stainless Steel (ASTM)

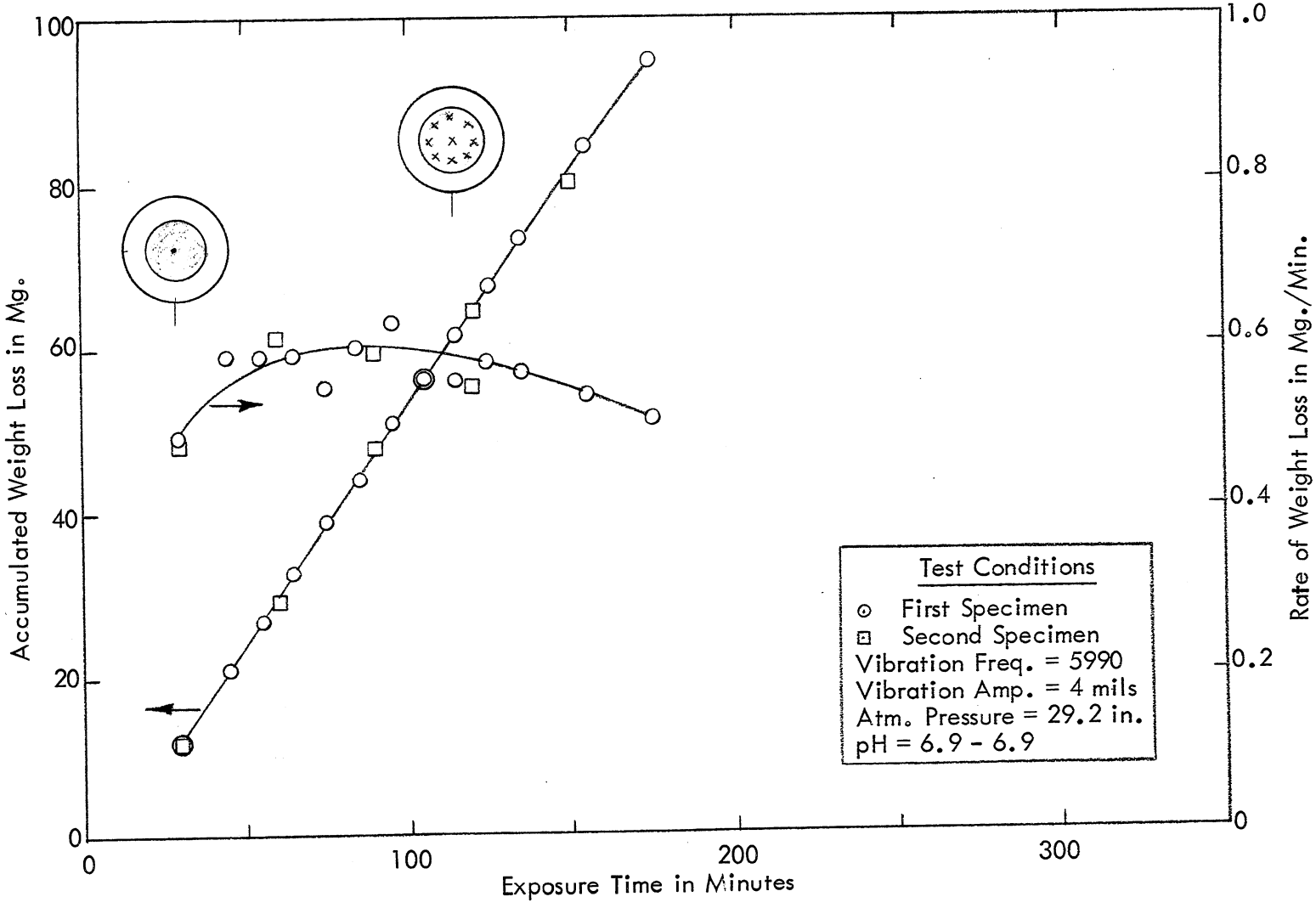

Fig. 4 Cavitation Erosion for 270 Nickel (ASTM)

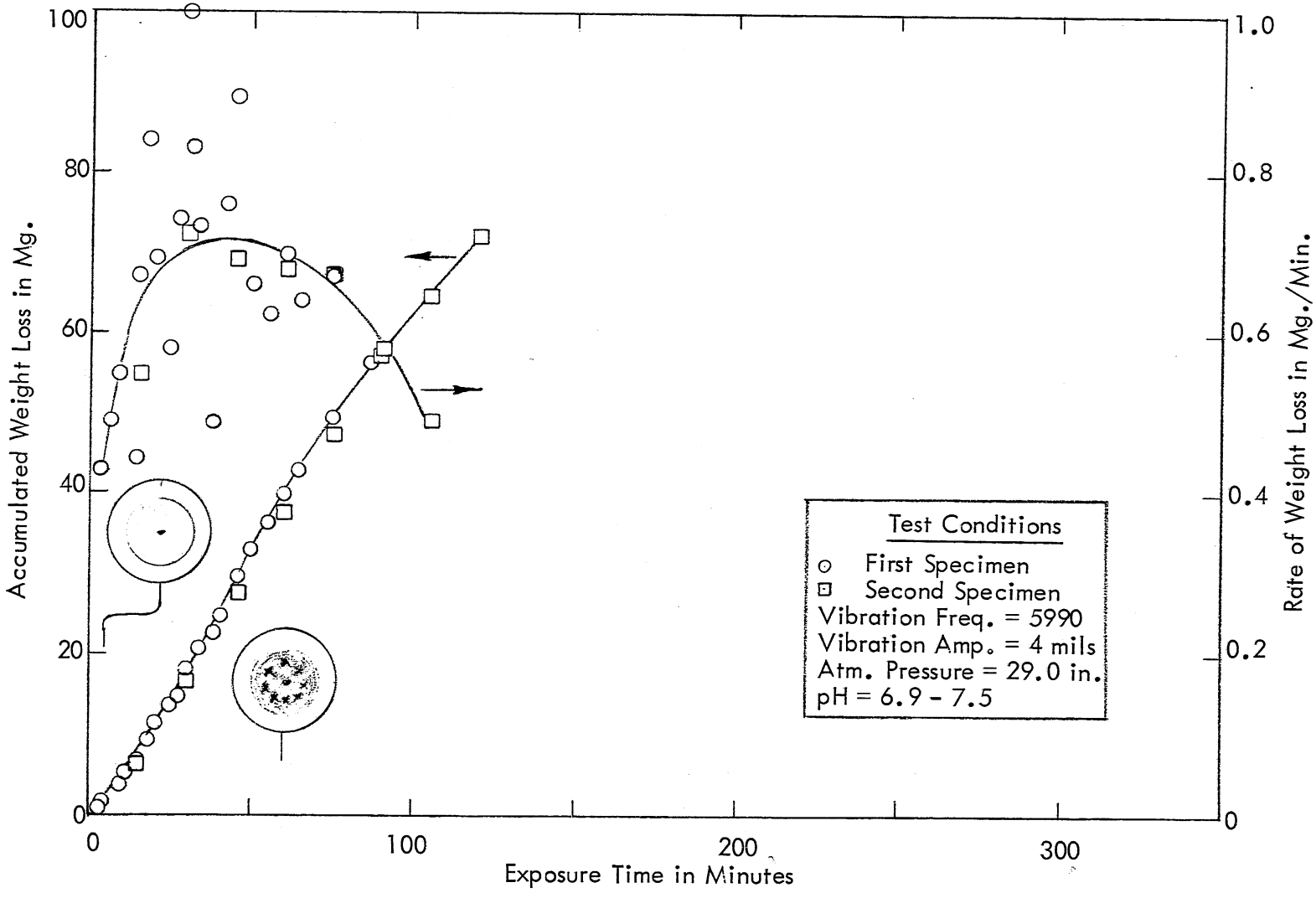

Fig. 5 Cavitation Erosion for Aluminum 6061 - T-651 (ASTM)

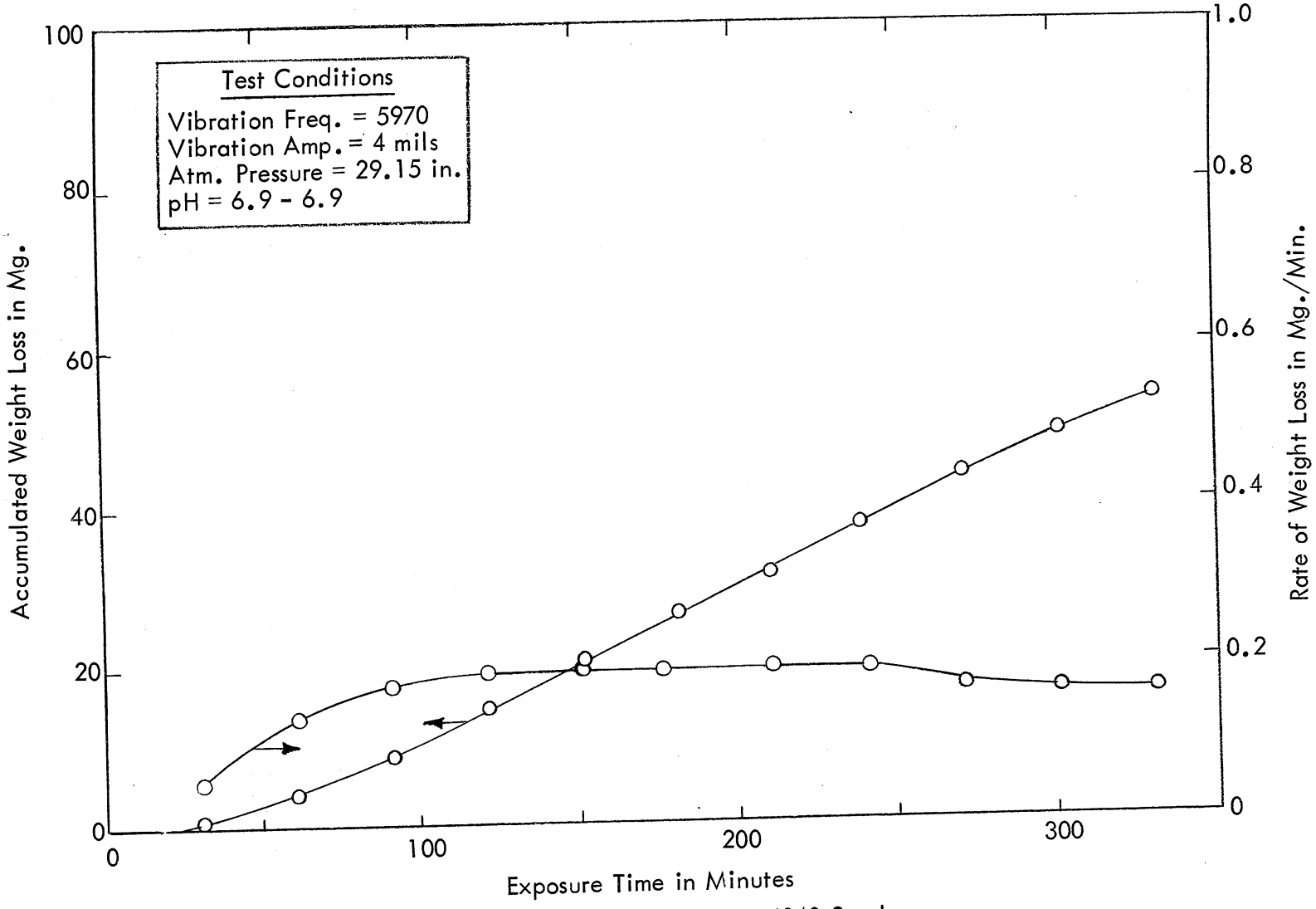

Fig. 6 Cavitation Erosion for 4340 Steel

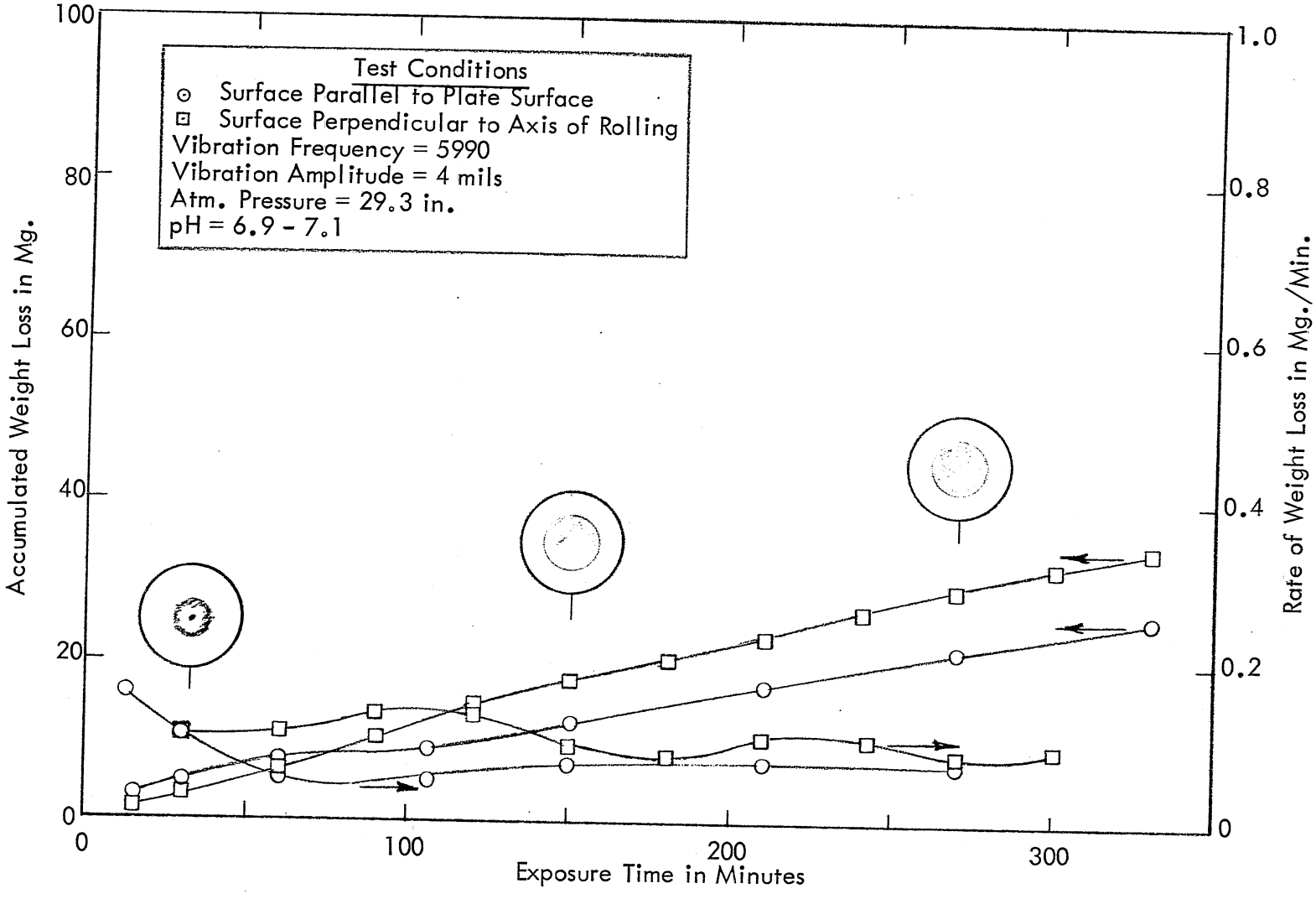

Fig. 7 Cavitation Erosion for 17-4PH Stainless Steel

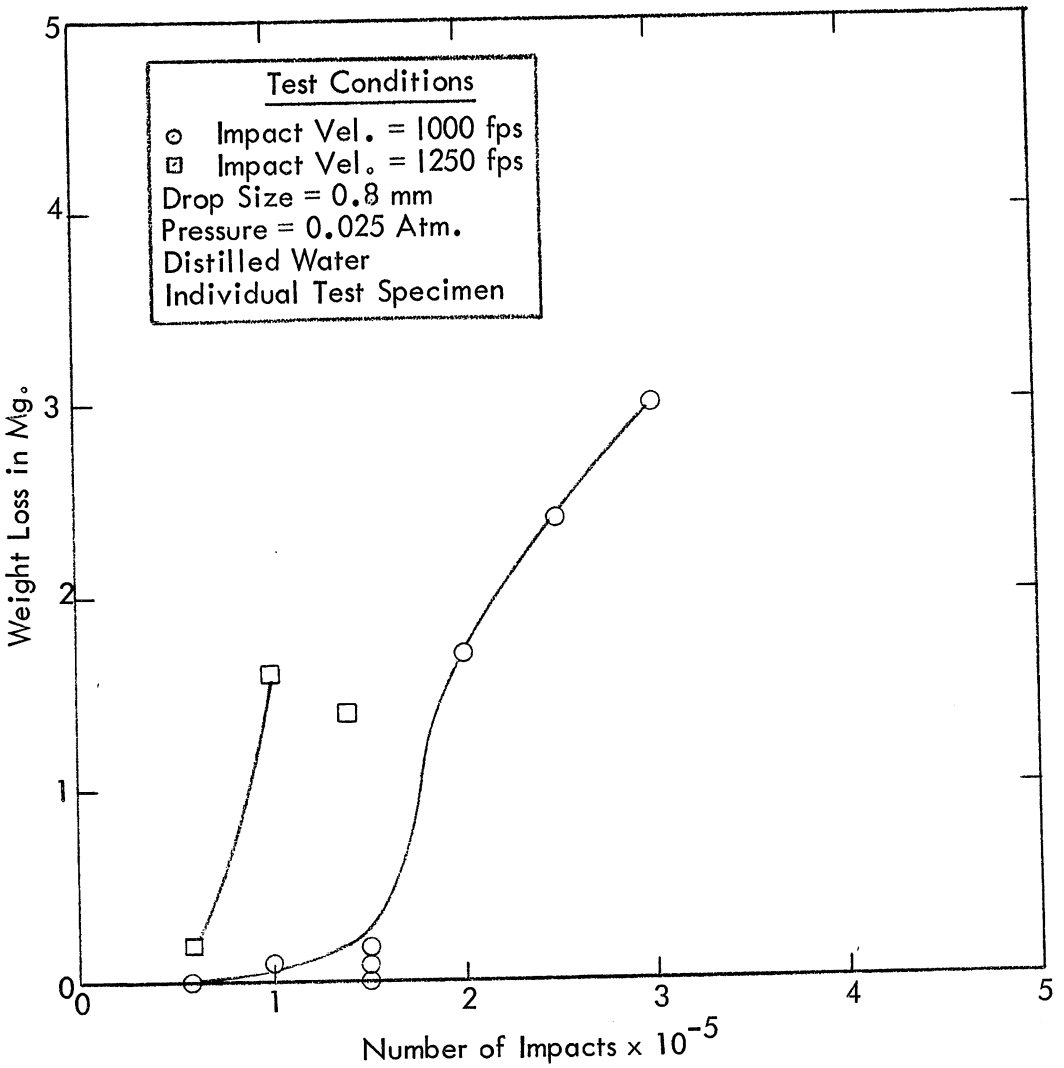

Fig. 8 Impingement Erosion for 316 Stainless Steel (ASTM)

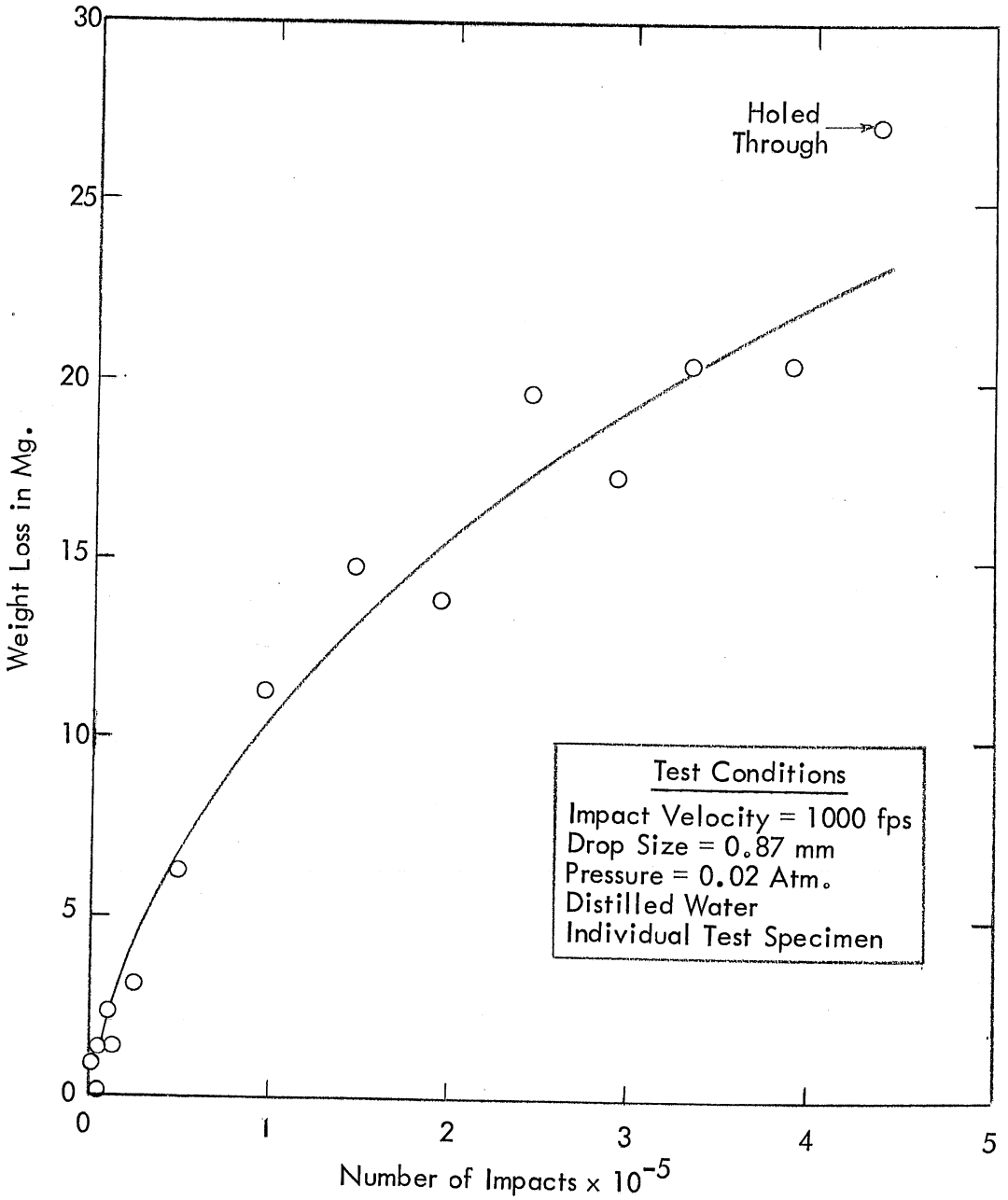

Fig. 9 Impingement Erosion for 270 Nickel (General Elect.)

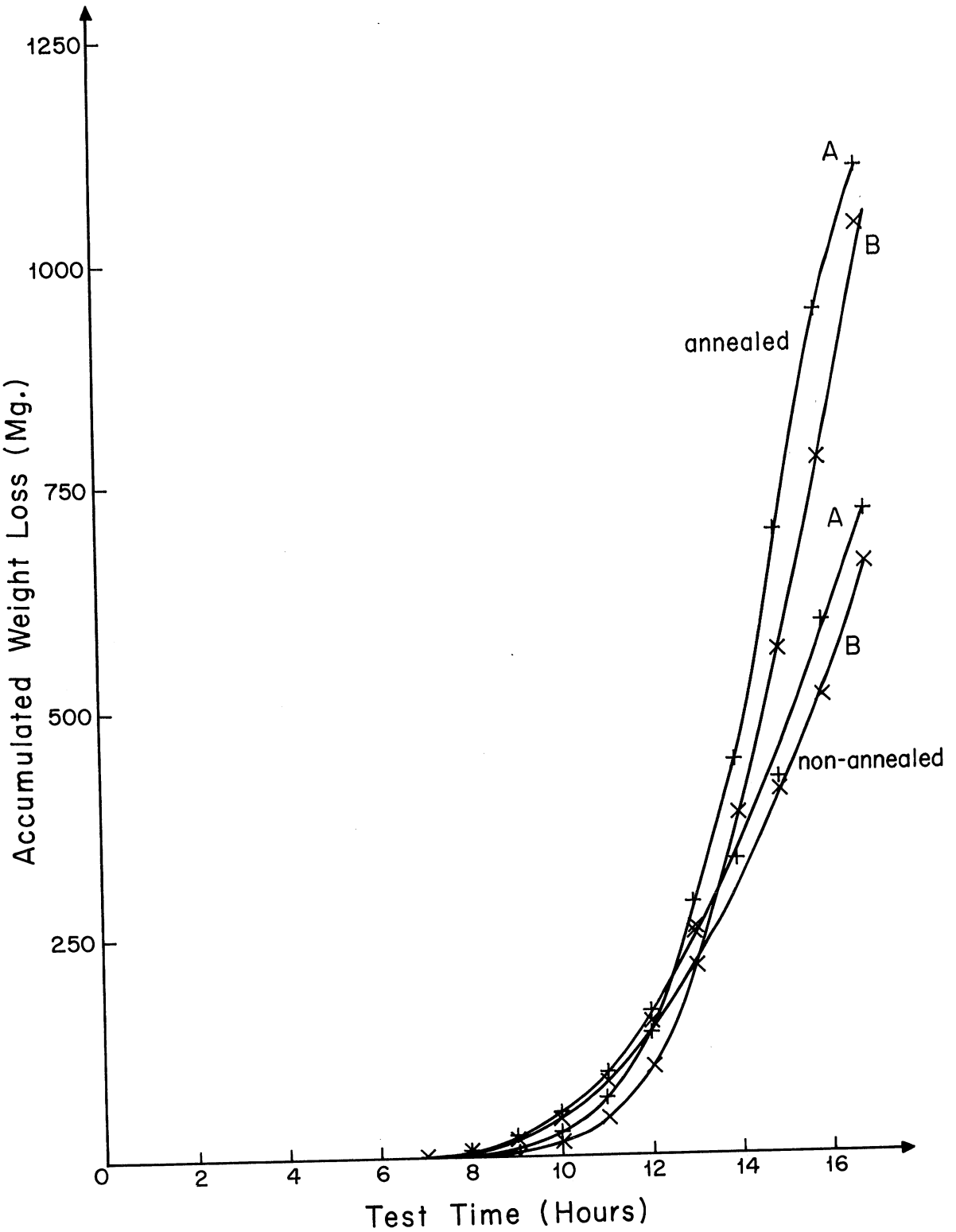

Fig. 10 Impingement Erosion for 316 Stainless Steel (ASTM)
(Tests by Electricite de France from Ref. [7])

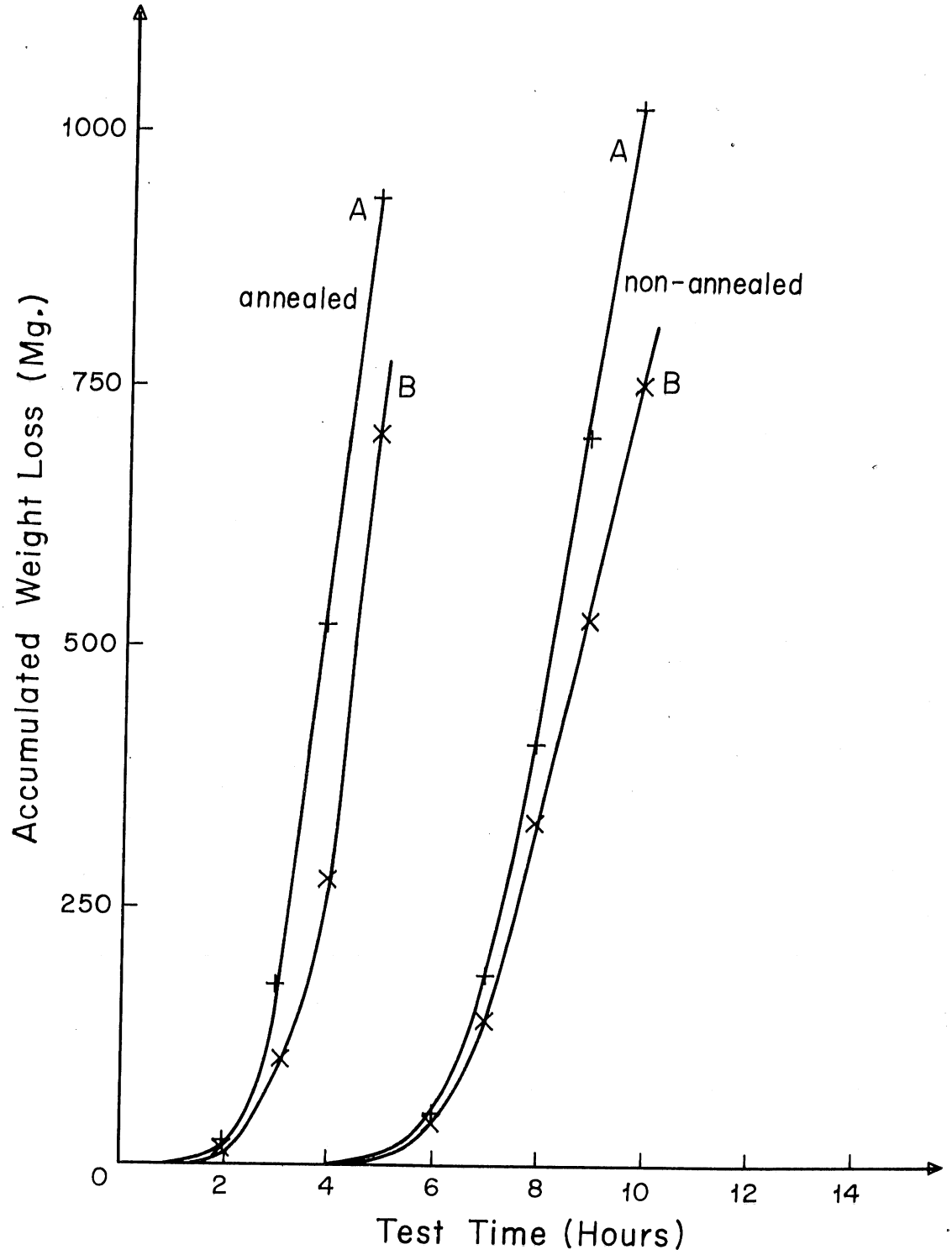

Fig. 11 Impingement Erosion for 270 Nickel (ASTM)
(Tests by Electricite de France from Ref. [7])

DISTRIBUTION LIST FOR PROJECT REPORT NO. 105
of the St. Anthony Falls Hydraulic Laboratory

Copies	Organization
40	Commander, Naval Ship Research and Development Center, Washington, D. C. 20007, Attn: 39 - Code L41 1 - Code 513
2	Commanding Officer, Naval Ship Research and Development Laboratory, Annapolis, Maryland 21402, Attn: Library
2	Commanding Officer, Naval Ship Research and Development Laboratory, Panama City, Florida 32402, Attn: Library
7	Commander, Naval Ship Systems Command, Department of the Navy, Washington, D. C. 20360, Attn: 1 - Code 0342 DEF 1 - Code 037 ADF 3 - Code 2052 1 - Code PMS 81 ABCDF 1 - Code 03412
20	Director, Defense Documentation Center, 5010 Duke Street, Alexandria, Virginia 22314
1	Chief of Naval Research, Department of the Navy, Washington, D. C. 20360, Attn: Mr. Ralph D. Cooper, Code 438
1	Director, Office of Naval Research Branch Office, 495 Summer Street, Boston, Massachusetts 02210
1	Director, Office of Naval Research Branch Office, 219 S. Dearborn Street, Chicago, Illinois 60604
1	Office of Naval Research Resident Representative, 207 West 24th Street, New York, New York 10011
1	Chief Scientist, Office of Naval Research Branch Office, 1030 East Green Street, Pasadena, California 91101
1	Director, Office of Naval Research Branch Office, 1076 Mission Street, San Francisco, California 94103
3	Commanding Officer, Office of Naval Research Branch Office, Box 39, Fleet Post Office, New York 09510
1	Commander, Naval Facilities Engineering Command, Department of the Navy, Washington, D. C. 20390, Attn: Code 0321 BCDE

Copies	Organization
6	Commander, Naval Ship Engineering Center, Department of the Navy, Center Building, Prince Georges Center, Hyattsville, Maryland 20782 Attn: Code 6110 Code 6114D Code 6120 AC Code 6132 CDE Code 6136 Code 6140 ADEF
1	Strategic Systems Projects Office, Department of the Navy, Washington, D. C. 20360, Attn: Dr. John Craven (NSP-001)
1	Commanding Officer, Naval Air Development Center, Johnsville, Warminster, Pa. 18974, Attn: Technical Library
11	Commanding and Director, Naval Applied Science Laboratory, Flushing and Washington Avenues, Brooklyn, New York 11251
2	Officer-in-Charge, Naval Undersea Warfare Center, 3202 E. Foothill Boulevard, Pasadena, California 91107, Attn: Dr. J. Hoyt AD Dr. A. Fabula AD
1	Commander, Naval Electronics Laboratory Center, San Diego, California 92152, Attn: Library DEF
1	Director (Code 2027), Naval Research Laboratory, Washington, D. C. 20390
1	Commanding Officer, Navy Underwater Weapons Research and Engineering Station, Newport, Rhode Island 02840
1	Commanding Officer and Director, Naval Civil Engineering Laboratory, Port Hueneme, California 93401, Attn: Code L31 DE
1	Commander D, Naval Weapons Center (Code 753), China Lake, California 93555
1	Commander, Boston Naval Shipyard, Boston, Massachusetts 02129, Attn: Technical Library
1	Commander, Charleston Naval Shipyard, Naval Base, Charleston, South Carolina 29408, Attn: Technical Library
1	Commander ABCF, Long Beach Naval Shipyard, Long Beach, California 90802, Attn: Technical Library
1	Commander, Norfolk Naval Shipyard, Portsmouth, Virginia 23709, Attn: Technical Library

Copies	Organization
1	Commander, Pearl Harbor Naval Shipyard, Box 400, Fleet Post Office, San Francisco, California 96610, Attn: Code 246-P
1	Commander, Philadelphia Naval Shipyard, Philadelphia, Pennsylvania 19112, Attn: Code 240 ABCF
1	Commander, Portsmouth Naval Shipyard, Portsmouth, N. H. 03801, Attn: Technical Library
1	Commander, Puget Sound Naval Shipyard, Bremerton, Washington 98314, Attn: Engineering Library
3	Commander, San Francisco Bay Naval Shipyard, Vallejo, California 94952, Attn: 1 - Technical Library 1 - Code 250 1 - Code 130Li BDF
1	AFFDL (FDDS - Mr. J. Olsen), Wright-Patterson AFB, Dayton, Ohio 45433 BDE
1	NASA Scientific and Technical Information Facility, P. O. Box 33, College Park, Maryland 20740
1	AFORSR (SREM), 1400 Wilson Blvd. BD, Arlington, Virginia 22209
1	Library of Congress, Science and Technology Division, Washington, D. C. 20540
1	U. S. Coast Guard, 1300 E Street N. W., Washington, D. C. 20591, Attn: Division of Merchant Marine Safety
1	Director, National Bureau of Standards D, Washington, D. C. 2034, Attn: Dr. G. B. Schubauer, Chief, Fluid Mechanics Branch
1	Director of Research, National Aeronautics and Space Administration, 600 Independence Avenue S. W., Washington, D. C. 20546 D
1	Director, Waterways Experiment Station, Box 631, Vicksburg, Mississppi 39180, Attn: Research Center Library BDE
1	Commander, Naval Ordnance Systems Command, Department of the Navy, Washington, D. C. 20360, Attn: Code ORD-035 D
1	Commandant (E), U. S. Coast Guard (Sta 5-2), 1300 E Street N. W., Washington, D. C. 20591
1	University of Bridgeport, Bridgeport, Connecticut 06602, Attn: Prof. Earl Uram Mech. Engr. Dept. ABDE

Copies	Organization
1	Brown University, Providence, Rhode Island 02912, Attn: Div of Applied Math D
4	Naval Architecture Department, College of Engineering, University of California, Berkeley, California 94720, Attn: 1 - Librarian 1 - Prof. J. R. Paulling 1 - Prof. J. V. Wehausen 1 - Dr. H. A. Schade
3	California Institute of Technology, Pasadena, California 91109, Attn: 1 - Dr. A. J. Acosta ABDE 1 - Dr. T. Y. Wu 1 - Dr. M. S. Plesset BDE
1	University of Connecticut, Box U-37, Storrs, Connecticut 06268, Attn: Prof. V. Scottron DE Hydraulic Research Lab
1	Cornell University, Graduate School of Aerospace Engr., Ithaca, New York 14850, Attn: Prof. W. R. Sears
1	Harvard University DE, 2 Divinity Avenue, Cambridge, Massachusetts, 02138, Attn: Prof. G. Birkhoff Dept of Mathematics
1	Pierce Hall D, Harvard University, Cambridge, Massachusetts 02138, Attn: Prof. G. F. Carrier
1	University of Illinois DE, College of Engineering, Urbana, Illinois 61801, Attn: Dr. J. M. Robertson Theoretical and Applied Mechanics Dept
1	The University of Iowa, Iowa City, Iowa 52240, Attn: Dr. Hunter Rouse
2	The University of Iowa, Iowa Institute of Hydraulic Research, Iowa City, Iowa 52240, Attn: 1 - Dr. L. Landweber 1 - Dr. J. Kennedy
1	The John Hopkins University, Mechanics Department, Baltimore, Maryland 21218, Attn: Prof. O. M. Phillips DF
1	Kansas State University DE, Engineering Experiment Station, Seaton Hall, Manhattan, Kansas 66502, Attn: Prof. D. A. Nesmith
1	University of Kansas D, Lawrence, Kansas 60644, Attn: Chm Civil Engr Dept

Copies	Organization
1	Lehigh University DE, Bethlehem, Pennsylvania 18015, Attn: Fritz Laboratory Library
1	Long Island University, Graduate Department of Marine Science, 40 Merrick Avenue, East Meadow, N. Y. 11554, Attn: Prof. David Price
1	Massachusetts Institute of Technology, Hydrodynamics Laboratory, Cambridge, Massachusetts 02139, Attn: Prof. A. T. Ippen DEF
7	Massachusetts Institute of Technology, Department of Naval Architecture and Marine Engineering, Cambridge, Massachusetts 02139, Attn: 1 - Dr. A. H. Keil 1 - Prof. P. Mandel ADE 1 - Prof. J. R. Kerwin 1 - Prof. P. Leehey DEF 1 - Prof. M. A. Abkowitz ABCDE 1 - Prof. F. M. Lewis D 1 - Dr. J. N. Newman ACD
1	U. S. Merchant Marine Academy, Kings Point, L. I., N. Y. 11024, Attn: Capt. L. S. McCready, Head, Dept. of Engineering AB
3	University of Michigan, Department of Naval Architecture and Marine Engineering, Ann Arbor, Michigan 48104, Attn: 1 - Dr. T. F. Ogilvie 1 - Prof. H. Benford 1 - Dr. F. C. Michelsen
5	St. Anthony Falls Hydraulic Lab., University of Minnesota, Mississippi River at 3rd Ave. S. E., Minneapolis, Minnesota 55414, Attn: 1 - Director 1 - Dr. C. S. Song 1 - Dr. J. M. Killen BDEF 1 - Mr. F. Schiebe DEF 1 - Mr. J. M. Wetzel DE
2	U. S. Naval Academy, Annapolis, Maryland 21402, Attn: 1 - Library 1 - Dr. Bruce Johnson ADF
2	U. S. Naval Postgraduate School, Monterey, California 93940, Attn: 1 - Library 1 - Prof. J. Miller D
1	New York University, University Heights, Bronx, New York 10453, Attn: Prof. W. J. Pierson, Jr.
2	New York University, Courant Institute of Mathematical Sciences DE, 251 Mercier Street, New York, New York 10012, Attn: 1 - Prof. A. S. Peters 1 - Prof. J. J. Stoker

Copies	Organization
2	University of Notre Dame, Notre Dame, Indiana 46556, Attn: 1 - Dr. A. Strandhagen BDE 1 - Dr. J. Nicolaides BD
2	The Pennsylvania State University, Ordnance Research Laboratory, University Park, Pennsylvania 15801, Attn: 1 - Drector ABDE 1 - Dr. G. Wislicenus ABDEF
1	Colorado State University, Department of Civil Engineering, Fort Collins, Colorado 80521, Attn: Prof. M. Albertson BDEF
1	Princeton University, Aerodynamics Laboratory, Department of Aerospace and Mechanical Sciences, the James Forrestal Research Center, Princeton, New Jersey 08540, Attn: Prof. G. Mellor DF
2	Scripps Institution of Oceanography, University of California, La Jolla, California 92038, Attn: 1 - J. Pollock 1 - M. Silverman ABCF
3	Stanford University, Stanford, California 94305, Attn: 1 - Prof. H. Ashley, Dept. of Aeronautics and Astronautics DE 1 - Prof. R. L. Street 1 - Prof. B. Perry, Dept. of Civil Engr.
3	Stevens Institute of Technology, Davidson Laboratory, 711 Hudson Street, Hoboken, New Jersey 07030, Attn: Dr. J. Breslin - 3
1	University of Texas, Defense Research Laboratory, P. O. Box 8029, Austin, Texas 78712, Attn: Director DF
1	University of Washington, Applied Physics Laboratory, 1013 N. E. 40th Street, Seattle, Washington 98105, Attn: Director ABDF
2	Webb Institute of Naval Architecture, Crescent Beach Road ABCD, Glen Cove, L. I., N. Y. 11542, Attn: 1 - Prof. E. V. Lewis 1 - Prof. L. W. Ward
1	Worcester Polytechnic Institute, Alden Research Laboratories, Worcester, Massachusetts 01609, Attn: Director ADE
1	Aerojet-General Corporation, 1100 W. Hollyvale Street, Azusa, California 91702, Attn: Mr. J. Levy, Bldg. 160, Dept. 4223
1	Bethlehem Steel Corporation, Central Technical Division, Sparrows Point Yard, Sparrows Point, Maryland 21219, Attn: Mr. A. Haff, Technical Mgr.
1	Bethlehem Steel Corporation ABC, Attn: H. de Luce, 25 Broadway, New York, New York 10004

Copies	Organization
1	Bolt Beranek and Newman Inc., 1501 Wilson Blvd., Arlington, Virginia 22209, Attn: Dr. F. Jackson DF
1	Bolt Beranek and Newman Inc., 50 Moulton Street, Cambridge, Massachusetts 02138, Attn: Dr. N. Brown A
1	Cornell Aeronautical Laboratory, Applied Mechanics Department, P. O. Box 235, Buffalo, New York 14221, Attn: Dr. I. Statler BDE
1	Electric Boat Division, General Dynamics Corporation, Groton, Connecticut 06340, Attn: Mr. V. Boatwright, Jr.
1	Esso International, 15 West 51st Street ABCD, New York, New York 10019, Attn: Mr. R. J. Taylor, Manager, R. and D Tanker Dept.
1	General Applied Sciences Laboratories Inc. DEF, Merrick and Stewart Avenues, Westbury, L. I., New York 11590, Attn: Dr. F. Lane
1	Gibbs and Cox, Inc., 21 West Street, New York, New York 10006, Attn: Technical Library
1	Grumman Aircraft Engineering Corporation, Bethpage, L. I., N. Y. 11714, Attn: Mr. W. Carl
2	Hydronautics, Inc., Pindell School Road, Howard County, Laurel, Maryland 20810, Attn: 1 - Mr. P. Eisenberg 1 - Mr. M. Tulin
1	Lockheed Missiles and Space Company, P. O. Box 504 AE, Sunnyvale, California 94088, Attn: Mr. R. L. Waid, Facility 1, Dept. 57-01, Bldg 150
2	McDonnell Douglas Aircraft Company, Douglas Aircraft Division DE, 3855 Lakewood Boulevard, Long Beach, California 90801, Attn: 1 - Mr. John Hess 1 - Mr. A. M. O. Smith
1	Measurement Analysis Corporation, 10960 Santa Monica Boulevard, Los Angeles, California 90025 DF
1	National Science Foundation, Engineering Division, 1800 G Street N. W., Washington, D. C. 20550, Attn: Director DE
1	Newport News Shipbuilding and Dry Dock Company, 4101 Washington Avenue, Newport News, Virginia 23607, Attn: Technical Library Dept.
1	Oceanics, Incorporated, Technical Industrial Park, Plainview, L. I., N. Y. 11803, Attn: Dr. Paul Kaplan

Copies	Organization
1	Pennsalt Chemicals Corporation, 900 First Avenue D, King of Prussia, Pennsylvania 19406, Attn: Mr. W. M. Lee, Director, Contract Res. Dept.
1	Robert Taggart, Inc., 3930 Walnut Street, Fairfax, Virginia 22030, Attn: Mr. Taggart
1	Sperry-Piedmont Company, Charlottesville, Virginia 22901, Attn: Mr. T. Noble
1	Society of Naval Architects and Marine Engineers, 74 Trinity Place, New York, New York 10006
2	Southwest Research Institute, 8500 Culebra Road BCDEF, San Antonio, Texas 78206, Attn: 1 - Dr. H. Abramson 1 - Applied Mechanics Review
1	Sun Shipbuilding and Dry Dock Co., Chester, Pennsylvania 18013, Attn: Mr. F. Pavlik ABC, Chief Naval Architect
1	Tracor Incorporated, 6500 Tracor Lane BDF, Austin, Texas 78721
1	TRG/ A Division of Control Data Corp., 535 Broad Hollow Road (Rt 110) Melville, L. I., N. Y. 11746
1	Woods Hole Oceanographic Institute, Woods Hole, Massachusetts 02543, Attn: Reference Room ABCDF
1	Prof. Jerome Lurye, Department of Mathematics, St. John's University ABCDE, Jamaica, New York 11432
1	Mr. B. H. Ujihara, North American Aviation Inc. BD, Space and Information Systems Div., 12214 Lakewood Boulevard, Downey, California 90241
1	Stanford Research Institute, Menlo Park, California 94025, Attn: Library
1	Cambridge Acoustical Associates, Inc., 129 Mount Auburn Street, Cambridge, Massachusetts 02138, Attn: Dr. M. C. Junger ABDF
1	Dr. Roland W. Jeppson, College of Engineering BDE, Utah State University, Logan, Utah 84321

Unclassified

Security Classification

DOCUMENT CONTROL DATA - R & D

(Security classification of title, body of abstract and indexing annotation must be entered when the overall report is classified)

1. ORIGINATING ACTIVITY *(Corporate author)*

St. Anthony Falls Hydraulic Laboratory
University of Minnesota

2a. REPORT SECURITY CLASSIFICATION

Unclassified

2b. GROUP

3. REPORT TITLE

COMPARATIVE STUDIES OF DROP IMPINGEMENT EROSION AND CAVITATION EROSION

4. DESCRIPTIVE NOTES *(Type of report and, inclusive dates)*

Final Report - October 1965 to April 1969

5. AUTHOR(S) *(First name, middle initial, last name)*

Ripken, John F.

6. REPORT DATE	7a. TOTAL NO. OF PAGES	7b. NO. OF REFS
April 1969	35	11

8a. CONTRACT OR GRANT NO.	9a. ORIGINATOR'S REPORT NUMBER(S)
Nonr 710(72) b. PROJECT NO. SR 009 01 01 c. d.	Project Report No. 105 9b. OTHER REPORT NO(S) *(Any other numbers that may be assigned this report)*

10. DISTRIBUTION STATEMENT

This document has been approved for public release and sale; its distribution is unlimited.

11. SUPPLEMENTARY NOTES	12. SPONSORING MILITARY ACTIVITY
	Naval Ship Research and Development Center

13. ABSTRACT

It has been theorized that the fundamental mechanism of cavitation erosion was essentially the same as that of impingement erosion. The tests conducted in this study were intended to provide additional cavitation and impingement data to support this theory. The tests were conducted on three materials supplied for an ASTM round-robin cavitation test program.

Complete cavitation tests and limited impingement tests on the three ASTM materials are described together with test data on two other metals. Further descriptive material on details for impingement testing is also included.

Only a limited comparison of cavitation and impingement erosion was possible with the data available. This suggests that accelerated laboratory erosion tests may, in fact, over-accelerate the erosion to such an extent that it is not possible to tie the observed erosion to the prototype problem.

DD FORM 1 NOV 65 1473 (PAGE 1)

S/N 0101-807-6811

Unclassified

Security Classification

A-31408

14. KEY WORDS	LINK A		LINK B		LINK C	
	ROLE	WT	ROLE	WT	ROLE	WT
Cavitation						
Erosion						
Damage						
Impingement						